Characterization of One-Dimensional Fiber-Optic Scintillating Detectors for Electron-Beam Therapy Dosimetry

Bongsoo Lee, Kyoung Won Jang, Dong Hyun Cho, Wook Jae Yoo, Sang Hun Shin, Gye-Rae Tack, Soon-Cheol Chung, Sin Kim, Hyosung Cho, Byung Gi Park, Joo Hyun Moon, and Siyong Kim

***Abstract*—In this study, a one-dimensional fiber-optic scintillating detector was developed for electron-beam therapy dosimetry. Each fiber-optic detector contains an organic scintillator as a sensitive volume and it is embedded and arrayed in a plastic phantom to measure one-dimensional high-energy electron-beam profiles of clinical linear accelerators. Plastic optical fibers guide the scintillating light which each detector probe generates to a photodiode array. The one-dimensional electron-beam profiles in the plastic phantom were measured in two different field sizes and for two electron-beam energies. Also, isodose and two-dimensional dose distributions in the plastic phantom were obtained using the one-dimensional scintillating detector array with two different electron beam energies.**

***Index Terms*—Cerenkov light, electron beam, fiber-optic detector, organic scintillator, plastic optical fiber.**

I. Introduction

MODERN radiotherapy dosimetry depends on the accuracy of radiation delivery to the target volume in the field of large-dose gradients and requires high-precision detectors in its dose measurements. Detectors should therefore be small enough for high spatial resolution in their dose measurements and have tissue-equivalent characteristics for accurate measurement without complex calibration processes [1]–[3]. Radiotherapy dosimetry also requires real-time and multi-dimensional measurements for dose distributions.

One-dimensional fiber-optic scintillating detectors for measuring high-energy electron beams can minimize dose distribution perturbation in plastic phantoms because the sensitive volume of these detectors is very small and nearly water-equivalent.

In this study, we have made one-dimensional fiber-optic scintillating detectors by using organic scintillators and plastic optical fibers (POFs) for high-energy electron-beam therapy dosimetry. Specifically, POFs are used to transmit a scintillating light generated by organic scintillators; also, photodiode arrays are used to convert light signals to electrical signals because they are compact, cheap, and easy to make in array form. Using these detectors, we have measured the intensities of scintillating light at two field sizes and two electron beam energies, and have obtained isodose curves for two different energy beams of a clinical linear accelerator (CLINAC).

We have also measured the intensity of Cerenkov light as a function of the incident angle of electron beams to investigate the influence of Cerenkov light on fiber-optic detectors. Cerenkov light produced in scintillators and in POFs usually causes problems in measuring real scintillating light signals, depending on the length of the optical fiber in the irradiation field and its angle in relation to the incident electron beam [4], [5]. Many methods have been developed and tested to solve this Cerenkov problem. However, it is known that tiny amounts of Cerenkov light can be detected when the angle between the incident electron beam and a fiber-optic detector is perpendicular [6].

Finally, we have measured two-dimensional dose distribution in a polymethylmethacrylate (PMMA) plastic phantom for 6 and 12 MeV electron-beam energies by using a one-dimensional scintillating fiber-optic detector.

II. Materials and Experimental Setup

POFs used in this study are step-index multimode fibers (CK-40, Mitsubishi Ltd., Tokyo, Japan). The outer diameter and the cladding thickness of these fibers are 1.0 mm and 0.02 mm, respectively. The refractive indices of the core and the cladding are 1.49 and 1.402, respectively, and the numerical aperture (NA) is 0.504. We used an organic scintillator synthesized with a polyvinyl-toluene (PVT) and wavelength-shifting fluors as a detector probe of the fiber-optic detector. It was found that typical organic scintillators, which are based on

Manuscript received November 14, 2007; revised June 11, 2008. Current version published December 04, 2008. This work was supported by the Basic Atomic Energy Research Institute (BAERI) program of the Ministry of Science and Technology (MOST; M20376030002-04B0505-00210).

B. Lee, K. W. Jang, D. H. Cho, W. J. Yoo, S. H. Shin, G.-R. Tack, and S.-C. Chung are with School of Biomedical Engineering, Research Institute of Biomedical Engineering, Konkuk University, Chungju 380-701, Korea (e-mail: bslee@kku.ac.kr; kko988@hotmail.com; bmecho@hanmail.net; wonzip@naver.com; ssh9431@paran.com; grtack@ kku.ac.kr; scchung@kku.ac.kr).

Sin Kim was with the Department of Nuclear and Energy Engineering, Applied Radiological Science Research Institute, Cheju National University, Cheju 690-756, Korea (e-mail: sinkim@cheju.ac.kr).

H. Cho is with the Basic Atomic Energy Research Institute and Department of Radiological Science, Yonsei University, Wonju 220-710, Korea (e-mail: hscho1@yonsei.ac.kr).

B. G. Park is with the Department of Energy and Environmental Engineering, Soonchunhyang University, Asan 336-745, Korea (e-mail: byunggi@ sch.ac.kr).

J. H. Moon is with Department of Energy and Environmental System Engineering, Dongguk University, Gyeongju 780-714, Korea (e-mail: jhmoon86@dongguk.ac.kr).

Siyong Kim is with the Department of Radiation Oncology, Mayo Clinic, Jacksonville, FL 32224 USA (e-mail: siyongkim@gmail.com).

Digital Object Identifier 10.1109/TNS.2008.2002578

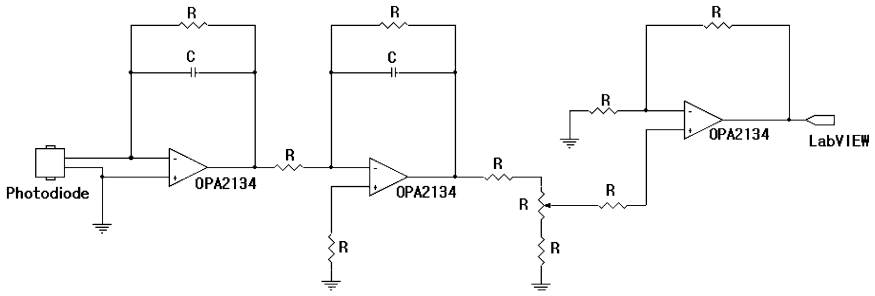

Fig. 1. Electric circuit of the photodiode amplifier system (R: resistance, C: capacitor).

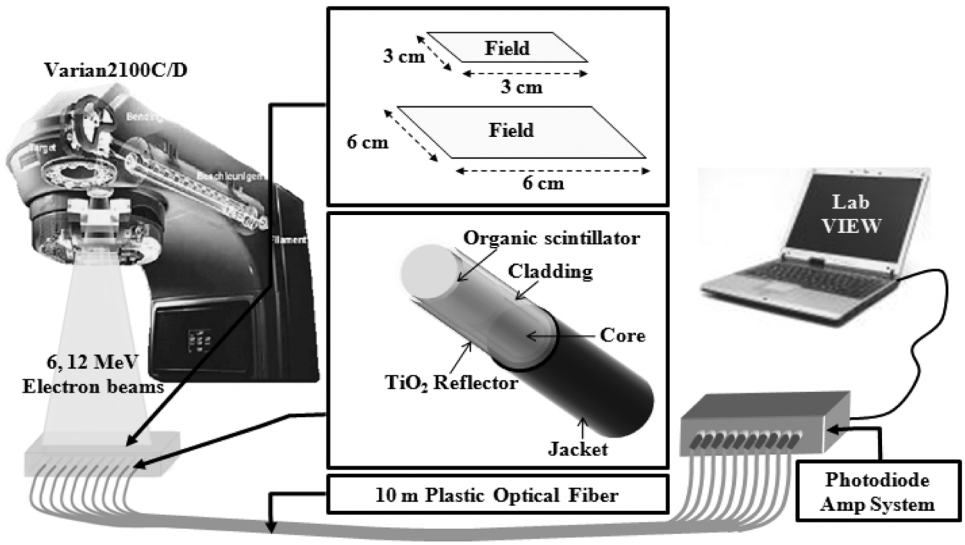

Fig. 2. Experimental setup.

PVT, show no signifying aging for absorbed doses up to 1.0 kGy [2]. This experiment used three kinds of commercially available organic scintillators (BCF-10, BCF-20 and BCF-60, Saint-Gobain Co., OH, USA) in order to select an organic scintillator which has more light output and is suitable for a light-measuring device. The physical properties of BCF-10 and BCF-20 are almost same, except for the wavelength of their peak emissions. These BCF-10s and BCF-20s can emit blue and green light with peak wavelengths of 432 nm and 492 nm, respectively. The decay time and the amount of emitted visible light of both organic scintillators are 2.7 nsec and about 8000 photons/MeV, but the emission peak and the decay time of BCF-60 are 530 nm and 7 nsec. Also, about 7100 photons/MeV are emitted during interactions with ionizing particles.

An organic scintillator with the diameter of 1 mm and the length of 10 mm was glued with an optical epoxy (DP-100 PLUS, 3M, MN, USA) to a 10-m length POF. The surfaces of both the scintillator and the POF were polished with various kinds of polishing pads in a regular sequence. The surface of the fiber-optic detector probe was surrounded by reflective-paint-based titanium oxide $(\mathrm{TiO_2})$ to increase the scintillating light-collection efficiency and to intercept light noise from outside. Fiber-optic detector probes were embedded in PMMA to make a one-dimensional detector array, and were connected to a photodiode (S1336-18BK, Hamamatsu Photonics Co., Hamamatsu, Japan) array by using POFs. It was reported that no significant degradation in the POF attenuation was observed for irradiations up to 3.5 kGy [5]. The usable wavelength range of the photodiode amplifier system is from 320 nm to 1100 nm with a peak wavelength of 960 nm, as a light-measuring device. The quantum efficiency (QE) of a photodiode is commonly expressed in percent (%) and has the following relationship with the photo-sensitivity (S) at a given wavelength (λ) [7]:

$$QE(\%) = \frac{S \times 1240}{\lambda} \times 100 \tag{1}$$

where, S is the photo-sensitivity in A/W at a given wavelength and λ is the wavelength in nm. The S of a photodiode used in this study is about 0.26 A/W at the emission peak of BCF-20 (492 nm) and the QE of a photodiode is about 65.5%. Fig. 1 shows electric circuit of the photodiode amplifier system. This homemade photodiode amplifier system is used to obtain a large signal-to-noise ratio with simple electronics. The amplification ratio is variable with resistors which are used in the amplifier circuit and the maximum amplification ratio is about 300 times.

Fig. 2 shows the experimental setup for measuring scintillating light using the one-dimensional fiber-optic detector array with the photodiode-amplifier system. Depending on its design, a CLINAC provides multiple numbers of electron energies with a typical range of 4 to 20 MeV. However, the most commonly used energy range is from 6 to 12 MeV. In this study, therefore,

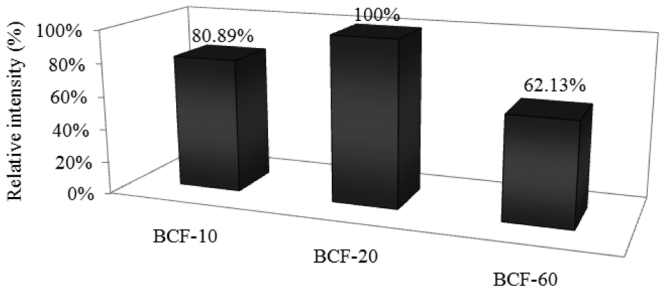

Fig. 3. Measurements of scintillating light outputs from different kinds of organic scintillators.

two electron beams (6 and 12 MeV) from the Varian CLINAC 2100CD were used. The field sizes of electron beams were 3 cm × 3 cm and 6 cm × 6 cm.

III. Results

Fig. 3 shows the measured scintillating light signals from three kinds of organic scintillators, the BCF-10, the BCF-20, and the BCF-60 with the 12 MeV electron beam. We selected the BCF-20 as probe material due to its high light output and short decay time. The relative light outputs of BCF-10 and BCF-60 to BCF-20 were about 81 and 62%, respectively for the 12 MeV electron beam with a 10 cm × 10 cm field size, as shown in Fig. 3.

Generally, the intensity of Cerenkov light generated in an optical fiber itself depends on the field size of the irradiation beam, the refractive index of the optical fiber material, and the incident angle between the electron beam and the optical fiber. The most dominant factor for deciding the intensity of Cerenkov light is the incident angle. Theoretically, the maximum Cerenkov transmission in PMMA occurs at the angle of 47.7° for 6 MeV electron beams [5]. The angle of maximum Cerenkov transmission increases only slightly as the electron energy increases above 4 MeV. It also increases as the refractive index of the medium increases.

In our previous work, we detected insignificant amounts of Cerenkov light when the angle between incident electron beam and the detector was perpendicular, and we could ignore the influence of Cerenkov light on detecting scintillating light with the fiber-optic detector when the incident angle was perpendicular [5]. Also, we expect to disregard the influence of Cerenkov light on the detection of scintillating light throughout this study because we used small field sizes of 3 cm × 3 cm and 6 cm × 6 cm, which caused no significant variations of incident angle through the whole field.

Fig. 4 shows the measured scintillating light signals from the one-dimensional fiber-optic detector array with different electron energies and irradiation field sizes. Fiber-optic detectors were placed in the depth of 1 cm of the PMMA phantom. The measured light signals show almost the same values and are distributed uniformly over field sizes of 3 cm × 3 cm and 6 cm × 6 cm for 6 and 12 MeV electron-beam energies. The results at 3 cm × 3 cm field sizes in Fig. 4(a) and (b) show that due to the reduced field size, only six detectors can measure distinct signals.

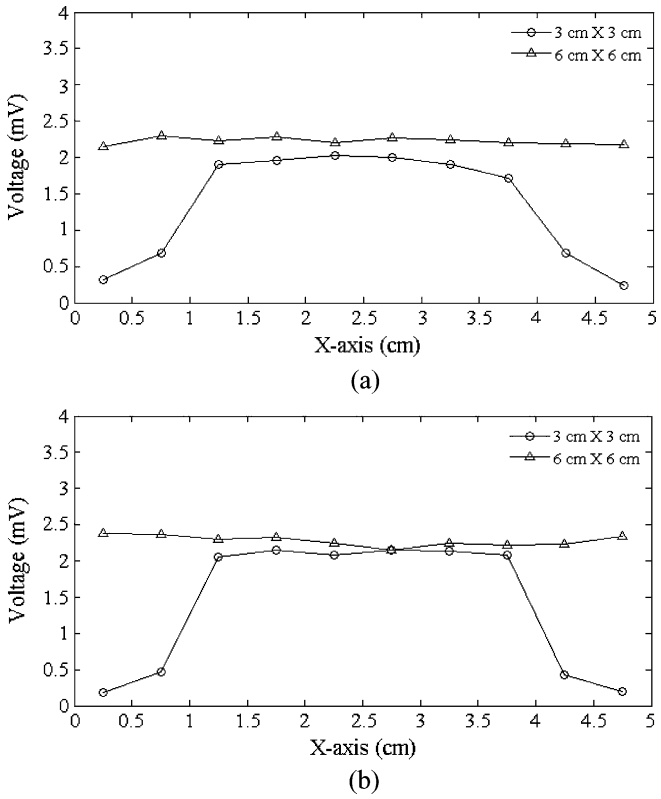

Fig. 4. Measurements of scintillating light using a one-dimensional fiber-optic detector array with 3 cm × 3 cm and 6 cm × 6 cm field sizes of two different energy electron beams ((a) 6 MeV, (b) 12 MeV electron beams).

Fig. 5 shows measured isodose curves for two different energy beams using the one-dimensional fiber-optic detector array. Generally, isodose curves describe the dose distributions in two dimensions, and are particularly useful tools for representing dose distributions for specific combinations of field size and beam energy. We placed 10 fiber-optic detectors with a gap of 0.5 cm in the PMMA phantom and measured the intensities of scintillating light at different depths of the phantom. The irradiation field size was 3 cm × 3 cm, and the source-surface distance (SSD) was 100 cm. For the 6 MeV electron beam, as shown in Fig. 5(a), all the isodose curves show some expansion and only the low isodose levels bulge out for the 12 MeV electron beam, as shown in Fig. 5(b) [8].

Fig. 5 also shows the depth of maximum dose increases with increase of the energy of the incident electron beams; the tissue penetration depths are about 3 cm and 6 cm for the 6 and 12 MeV electron beams, respectively. We know that the penetration depth may be estimated roughly with the following expression [9]:

$$Penetration\ depth(\mathrm{cm}) = \frac{electron\ energy(\mathrm{MeV})}{2(\mathrm{MeV/cm})}. \quad (2)$$

Compared with the isodose curves of a photon beam, the field size for an electron beam expands rapidly below the surface of a phantom because electrons scatter rapidly as the electron beam penetrates the medium.

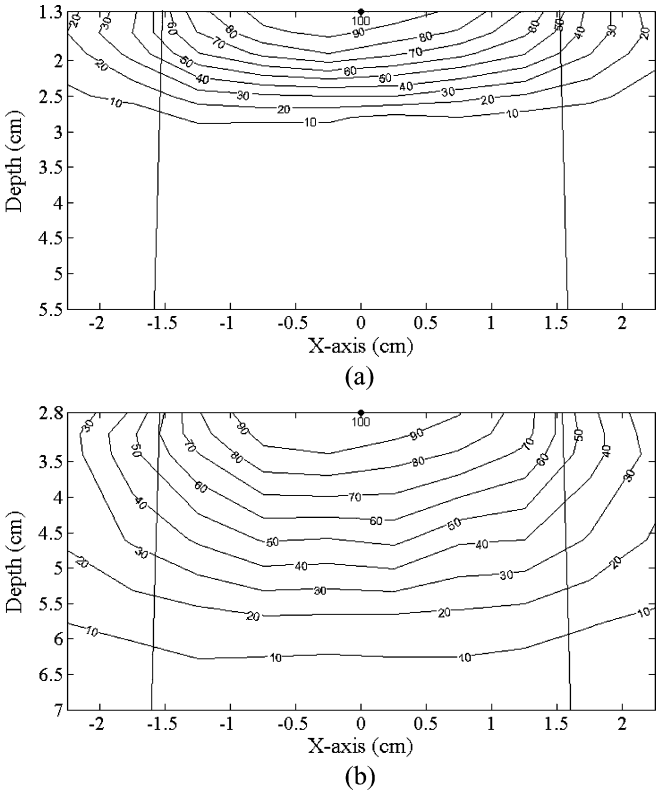

Fig. 5. Measurements of isodose lines using a one-dimensional fiber-optic detector array with a 3 cm × 3 cm field size of two different energy electron beams [(a) 6 MeV, (b) 12 MeV electron beams].

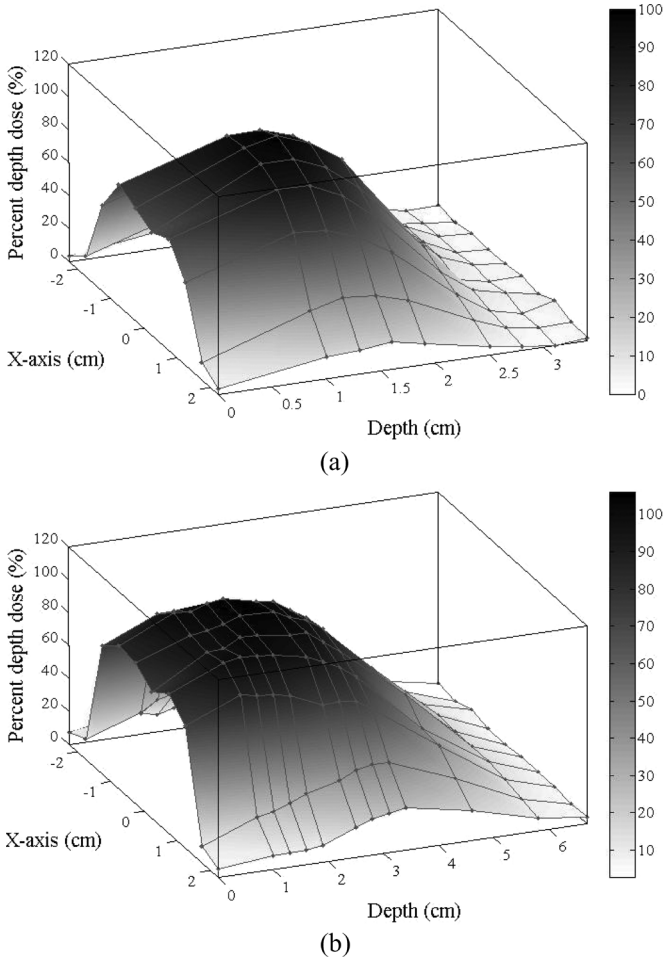

Fig. 6. Measurements of two-dimensional dose distributions in the 3 cm × 3 cm field for two different energy electron beams [(a) 6 MeV, (b) 12 MeV electron beams].

In clinical practice, the central axis dose distribution is characterized by percent depth dose (PDD) which can be defined as the quotient of the absorbed dose at any depth t (d_t) to the absorbed dose at a fixed reference depth t_o (d_{to}). PDD can be expressed as [8]:

$$PDD(\%) = \frac{d_t}{d_{t0}} \times 100. \tag{3}$$

For high-energy electron beams, the reference depth is usually taken at the position of the peak absorbed dose. The peak absorbed dose on the central axis is called the $\mathrm{d}_{\max}$ which is defined by the following expression:

$$d_{\max} = \frac{d_t}{PDD} \times 100. \tag{4}$$

Fig. 6 shows two-dimensional dose distributions obtained from profile measurements at multiple depths in the 3 cm × 3 cm field for 6 (a) and 12 (b) MeV electron beams. As given in (3), PDD is the ratio of dose at depth to dose at a fixed reference depth, expressed in percentage, and it varies according to SSD, energy, and field size. It has been observed that the typical depths of maximum dosage along the central axis for 10 cm × 10 cm field in a water phantom are about 1.3 cm and 2.8 cm, for 6 and 12 MeV electron beams, respectively [8].

In Fig. 6, the $\mathrm{d}_{\max}$ along the central axis is 1.3 cm for the 6 MeV electron beam. For the 12 MeV electron beam, $\mathrm{d}_{\max}$ is in the range of 2 to 3 cm. It is more difficult to find $\mathrm{d}_{\max}$ for higher electron beam energies, as the dose builds up more slowly and over a longer distance at the higher energies.

IV. Conclusion

In this study we fabricated a one-dimensional fiber-optic detector array using an organic scintillator for high-energy electron-beam therapy dosimetry. We also measured one-dimensional beam distributions in a PMMA phantom with two different energies and field sizes of electron beams using a fiber-optic detector and obtained isodose curves and two-dimensional dose distributions for high-energy electron beams. Through this study, we obtained many reasonable results such as penetration depths, isodose curves, and PDDs. They are consistent with well known data which are measured using conventional dosimeters in radiotherapy.

The newly developed one-dimensional fiber-optic detector array has many advantages over conventional dosimeters in electron beam therapy. First, water-equivalent organic scintillators, POFs and the PMMA phantom make it possible to measure dose distribution with a minimal perturbation. Second, small sensitive volume of these detectors can contribute to dose-distribution measurements with a high resolution. Third, the one-dimensional multichannel measurements system would

be used for quality assurance purposes for electron beam therapy with reduced time. Especially, this one-dimensional dose measurements system allows us to obtain depth dose curves in a very short time. Fourth, real-time measurements also can not only save time but also give chances of real-time feedback for quality assurance. Fifth, there should be no corrections such as temperature, pressure or humidity for accurate dose measurements in the fiber-optic detector array. This new one-dimensional fiber-optic detector can be expected to be effective for measuring dose distributions (i.e., isodose curves) and PDDs in electron beam therapy dosimetry.

REFERENCES

[1] A.-M. Frelin, J.-M. Fontbonne, G. Ban, J. Colin, and M. Labalme, "Spectral discrimination of Cerenkov radiation in scintillating dosimeters," *Med. Phys.*, vol. 32, pp. 3000–3006, 2005.

[2] T. O. White, "Scintillating fibers," *Nucl. Instrum. Methods Phys. Res. A.*, vol. A273, pp. 820–825, 1988.

[3] A. S. Beddar, "Plastic scintillation dosimetry and its application to radiotherapy," *Radiat. Meas.*, vol. 41, pp. S124–S133, 2007.

[4] M. A. Clift, R. A. Sutton, and D. V. Webb, "Dealing with Cerenkov radiation generated in organic scintillator dosimeters by Bremsstrahlung beams," *Phys. Med. Biol.*, vol. 45, pp. 1165–1182, 2000.

[5] B. Lee, D. H. Cho, K. W. Jang, S. C. Chung, J. W. Lee, S. Kim, and H. Cho, "Measurements and characterizations of Cerenkov light in fiber-optic radiation sensor irradiated by high energy electron beam," *Jpn. J. Appl. Phys.*, vol. 45, no. 10A, pp. 7980–7982, 2006.

[6] B. Lee, K. W. Jang, D. H. Cho, W. J. Yoo, G. R. Tack, S. C. Chung, S. Kim, and H. Cho, "Measurements and elimination of Cherenkov light in fiber-optic scintillating detector for electron beam therapy dosimetry," *Nucl. Instrum. Methods Phys. Res. A.*, vol. A579, pp. 344–348, 2007.

[7] Selection Guide of Si Photodiodes, Hamamatsu Photonics Co., Hamamatsu, Japan, p. 32, 2006.

[8] F. M. Khan, *The Physics of Radiation Therapy*, 2nd ed. Baltimore, MD: Williams & Wilkins, 1994, pp. 179–371.

[9] W. R. Hendee, G. S. Ibbott, and E. G. Hendee, *Radiation Therapy*, 3rd ed. New York: Wiley, 2005, pp. 151–152.